Enhancing Reliability of Photovoltaic Power Electronic Converters Under Dynamic Irradiance Conditions

Renato Jacobo Tapia, Mahmoud Shahbazi

Durham University, Durham, UK

Abstract

This paper presents a novel temperature-controlled maximum power point tracking (MPPT) algorithm for lifetime improvement of a photovoltaic (PV) converter under dynamic irradiance conditions. The proposed algorithm controls and limits the junction temperature change rate of switching devices, reducing the thermal stress and drastically reducing the damage received, hence improving the reliability and lifetime of power converters in PV systems. To evaluate the damage reduction, a lifetime estimation technique is applied which is composed of a Foster thermal model, a rainflow counting algorithm and an empirical lifetime model. Moreover, in this paper the energy and life consumption are calculated with the application of lookup tables to reduce computation time. The effectiveness of the proposed algorithm is verified using extensive simulations and by comparing energy generated and life consumption under irradiance profiles for different cloud conditions. The temperature-controlled algorithm is applied in parallel with a normal MPPT algorithm to a 10 kW photovoltaic system and results are compared using irradiance data from the province of Quebec, Canada to validate its efficacy. The obtained results show that for very variable cloud conditions, the modified algorithm managed to reduce the life consumption by 4.68% at no extra cost, with just 0.08% of energy generation reduction, proving its effectiveness.

Keywords: Thermal management, MPPT, Power electronic, Reliability, Lifetime evaluation.

1 Introduction

Power electronics has an increasing role in energy generation and management. It has improved the efficiency of electric systems and allowed more flexible control of power conversion systems. However, reliability has become one major issue for power electronic systems as it affects their cost and life expectancy [1][2]. For many applications, the working environments are full of stressors (e.g. humidity, high temperature, vibrations, temperature cycling, dust) which threaten reliability and can lead to early failures [1][3]. This is especially true for renewable energy systems that work in harsh environments. To overcome these issues, the industry has changed to a Design for Reliability (DfR) process [4] where the reliability study is executed during the design phase of power electronics systems instead of testing afterwards. By this means the reliability of power electronics systems can be improved without compromising cost and security.

Photovoltaic (PV) energy has seen a sharp growth in recent years [1]. Although PV energy seems promising, it may face problems in some operation environments thus these systems can benefit from the application of DfR. In PV systems, the inverter accounts for 37% of failures and from these failures, 21% are caused by problems with power semiconductors [5], making them a significant source of reliability issues. Also, in surveys from industry experts, power semiconductors were identified out as the most critical components [6]. What is more is that the inverter failures in PV systems account for 58% of maintenance costs [7], and therefore improving reliability levels and reducing failure rates would reduce maintenance cost as PV inverters are costly. Overall, it is evident that PV converters are the root of reliability issues in PV systems, and therefore, significant cost reduction in PV systems might be achieved by enhancing the reliability and lifetime of these converters [8].

The reliability and lifetime of power converters is shown to be mainly impacted by the thermal cycles experienced by their semiconductors [1], caused by energy loss during their operation [9]. For example, one of the principal failure mechanisms in insulated-gate bipolar transistors (IGBTs) devices is bond-wire fatigue caused by cycling variations in junction temperature (T_j) and temperature difference (ΔT_j) [10]. These thermal cycles are in turn greatly influenced by solar irradiance and therefore cloud conditions, as well as ambient temperature, which are the main components of a PV mission profile [11]. Another issue that affect the reliability of PV converters is the constant variations of irradiance during days with passing clouds [12]. In a day with clear sky, the solar irradiance affects the reliability of the system in the form of available power due to power losses in the IGBT devices. For days with dynamic cloud conditions, the constant change in solar irradiance and available power leads to further thermal cycling.

Many recent studies have tried to investigate the impact of mission profile on the reliability of PV power converters and to propose ways of increasing the reliability and lifetime of the converters. For example, the impact of modulation scheme, mission profile and PV array configuration on the reliability of a double-stage single-phase PV inverter is studied in [1]. However, impact of could conditions (solar irradiance), or a modification of MPPT algorithm are not considered here. In [15] the application of an optimized maximum power point tracking (MPPT) algorithm is discussed, where the algorithm controls the temperature change rate of PV systems, resulting in lifetime improvement and a slight power reduction. This study, however, does not include a field operation mission profile verification. Power Limiting Control (PLC) is another approach that has been studied in several works in recent years for extending the lifetime of converters . These methods work by limiting the maximum input power to a certain level, hence reducing the thermal variations at the expense of reduced power handling capability. The works in [8] and [13] rely on a power limitation to regulate the lifetime impact on PV system. To achieve this, the MPP tracking is shifted by regulating the required input voltage of the converter based on the maximum power allowed. Active thermal control for power modules and the trade-off between lifetime extension and cost due to efficiency reduction is studies in [14]. However, none of these methods consider variable cloud conditions, and therefore they are inherently ineffective against thermal cycling induced by these conditions.

In particular, the effect of cloud conditions on the lifetime of PV systems has not been considered adequately. Cloud conditions have a significant effect on the irradiance that a PV system will receive. Clouds cause fluctuating irradiance conditions, that lead to temperature cycles in PV systems [16], which reduce the expected lifetime. Mitigation of such cycles can be achieved by the implementation of temperature-controlled MPPT algorithms, improving the reliability and lifetime of the system.

To address this gap, this paper first studies the impact that different irradiance variation conditions have on the reliability of the system and carries out detailed analysis of the effect of dynamic irradiance conditions on the reliability and lifetime of power semiconductors in PV converters. Secondly, this paper also proposes a new temperature-controlled MPPT algorithm to improve the lifetime of PV systems under these dynamic irradiance conditions, at no extra cost. The presented method is the first to consider variable solar irradiance conditions and is shown to be effective against temperature cycling caused due to these conditions. Moreover, it offers a simple design, which makes it suitable for a wide range of controllers. The study includes a lifetime analysis of IGBT devices as critical components of PV systems for a DfR. The system is tested under mission profiles that a PV system might encounter in field operation. The irradiance profiles comprise different cloud conditions (clear day, overcast day, variable and very variable cloud conditions), which are selected to analyze the performance of the system and the impact of the algorithm on lifetime improvement. The system operation of a PV system is performed and studied under the control of a normal MPPT algorithm in parallel with a modified temperature-controlled MPPT algorithm for a cloud condition reliability assessment.

The remainder of the paper is organised as follows: in Section 2.1 an empirical lifetime estimation technique is described, which includes the estimation of power losses of the IGBT devices in the system, a thermal model that represents the temperature endured by the IGBTs, along with a rainflow algorithm for the counting of thermal cycles and the lifetime model. Then, the proposed optimised MPPT algorithm is presented and explained in Section 2.2. Next, the simulation setup and characteristics are described in Section 3 along with the results and main findings. Finally, the conclusion of the study is expressed in Section 4.

2 Materials and Methods

2.1 Lifetime Model

This section explains the steps necessary for the application of a lifetime estimation method according the one presented in [17]. The lifetime of power converters depends on different components such as capacitors and semiconductors [5]. Power semiconductors were highlighted as the most crucial elements of the system [6]. For this reason and with the aim of simplicity, this work will focus on the analysis of the lifetime of IGBT devices.

There are different strategies to evaluate the lifetime of IGBTs [17]. The first group are failure rate methods, which depend on constant failure rates that do not consider temperature fluctuations and fail to faithfully represent the behaviour of PV systems that are affected by the environmental conditions. Next are empirical lifetime models, that depend on the statistical analysis of power cycling data of IGBT devices [18] that fail to express the specific failure mechanism. Finally, there are Physics of Failure (PoF) methods, which estimate the lifetime of IGBT devices based on the stress-strain deformation of bond wires due to thermal cycling. Although PoF methods can be effective, the main drawback of these methods is the limited knowledge of material characteristics and the layout of the IGBTs in each case study. For this reason, as well as the fact that that empirical lifetime models have good accuracy and can be easily implemented with information obtained from data-sheets, an empirical model is implemented for lifetime estimation in this paper.

The flow diagram in Fig. 1 shows the process of the lifetime estimation process, which is further explained in the rest of the section. First, an irradiance mission profile is fed into the electrical model of a PV system and the energy generated by the system and energy losses of the IGBT switches is determined. Next, the energy losses are used to estimate the temperature experienced by the IGBT devices during the mission profile using a thermal equivalent model [9]. Then, the temperature profile is processed by a rainflow counting algorithm that classifies the random temperature cycles [19]. Finally, the organized temperature cycles are used to evaluate the life consumption of the IGBT devices with the use of the Bayerer's model [18].

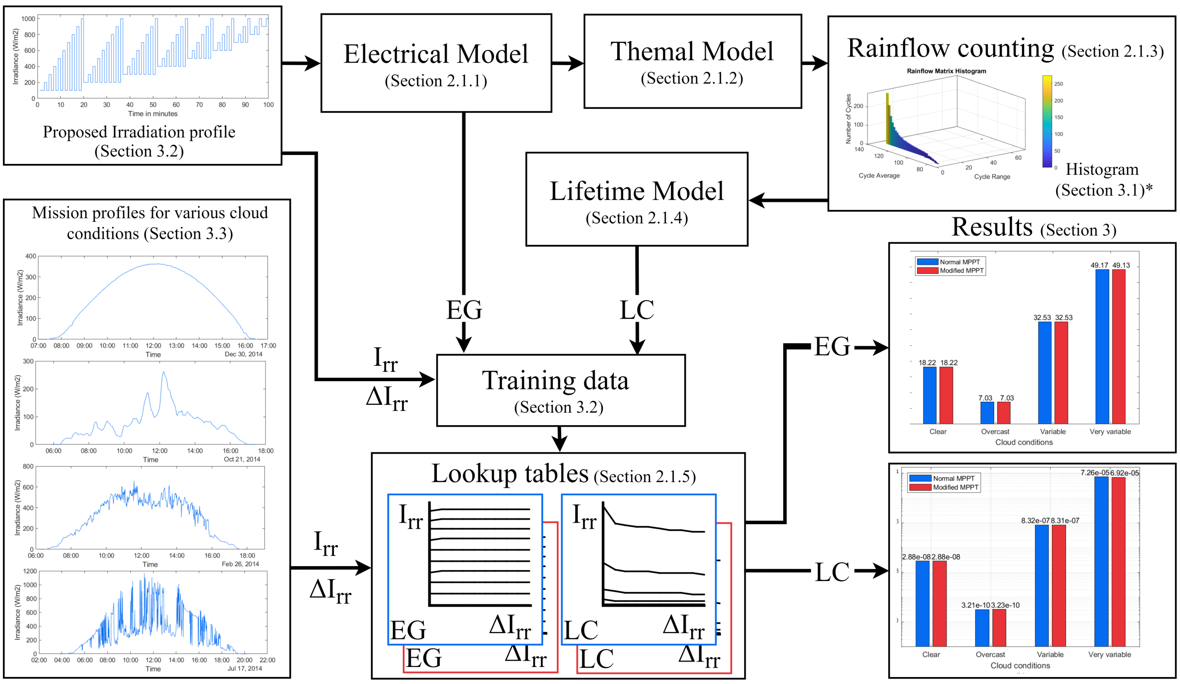

Figure 1: Flow diagram of the proposed method to estimate the life consumption and energy generated by the system. I_{rr} is the current irradiance level, ΔI_{rr} is the differential of the current and previous irradiance level, EG is the energy generated, and LC is the life consumption

2.1.1 Electrical model & power losses

For this study, a single-phase two-stage grid-connected PV converter is used. The first stage of the converter is a DC-DC boost converter controlled by a perturb & observe (P&O) MPPT algorithm, which regulates the power harvested by the system. The second stage is a full-bridge converter , which is synchronized to the grid with the use of a phase-locked loop (PLL). The V_{DC} controller makes sure that the DC link voltage remains controlled, and all energy extracted from the solar panels (barring losses) is therefore fed to the grid. The frequency and the phase angle of grid voltage are determined using the PLL. Using Park transformation and a synchronous frame, d and q components of the current are determined and regulated using two conventional PI controllers [20],[21]. The outputs of these controllers are used to determine the reference voltages for the PWM module.

The system configuration can be seen in Fig. 2. The parameters of the PV system will be defined in Section 3.

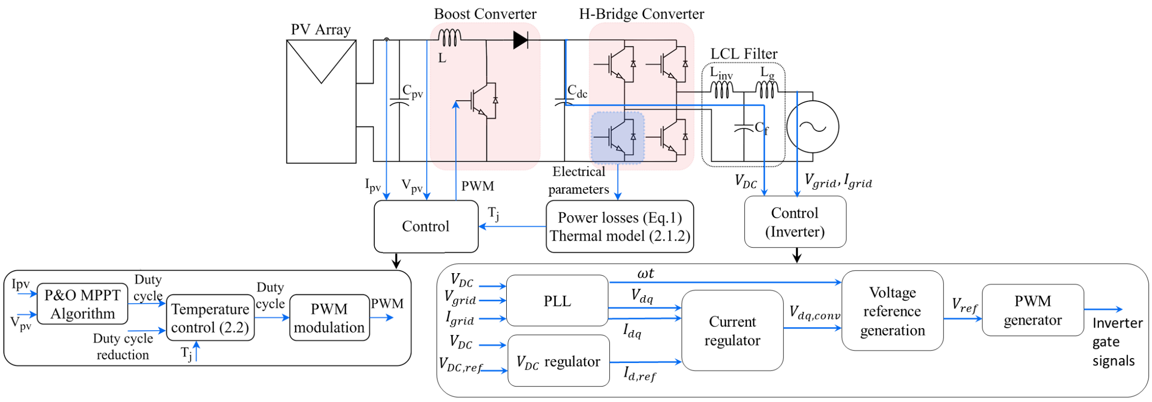

Figure 2: Electric diagram of a 2-stage 10 kW PV converter. The first stage is composed by a boost converter controlled by a MPPT algorithm, the second stage is a full-bridge grid-connected inverter. I_{pv} is the PV current, V_{pv} is the PV voltage, T_j is the junction temperature, C_{pv},C_{dc},C_f are the PV, DC-link and LCL filter capacitors respectively, L_{inv},L_g are the inverter side and grid side inductors of the LCL filter respectively. V_{DC} is the DC-link voltage, and I_{grid} and V_{grid} are the voltage and current at the grid connection, respectively

Both stages have an effect on the IGBT power losses; the first stage principally in the way of available power and the second stage in the way of sinusoidal current injection. The switch power losses (P_{losses}) are caused mainly by conduction losses (P_{cond}) and switching losses (P_{sw}) and can be evaluated with help of parametric measurements and specific data from the implemented switching devices.

$$P_{losses} = P_{cond} + P_{sw} \tag{1}$$

Conduction losses can be evaluated uisng the collector-emitter voltage (V_{ce}) and the collector current (I_c) of the IGBT devices:

$$P_{cond} = V_{ce} \cdot I_c \tag{2}$$

The switching losses (P_{sw}) occur from the transition of switches from blocking state to conduction state (E_{on}) and vice versa (E_{off}) and are dependent of the switching frequency (f_{sw}) of the system. The E_{on} and E_{off} parameters which are obtained from the data-sheet of the implemented device are used to evaluate the switching losses:

$$P_{sw} = (E_{on} + E_{off}) \cdot f_{sw} \tag{3}$$

2.1.2 Thermal model

The degradation of IGBT devices is linked to temperature fluctuations, therefore it is necessary to accurately estimate thermal variations to predict the lifetime of the switches. Energy dissipation during the operation of the system leads to variations in the temperature of the IGBTs, such variations of temperature can be estimated with the application of a thermal RC (Resistor-Capacitor) equivalent model. The RC thermal models are used to represent the physical thermal characteristics of materials.

There are two main types of thermal RC equivalent models, Cauer and Foster models. The cauer model is represented by a continued-fraction RC circuit which has the advantage of a more precise temperature modelling concerning all the materials and connection points of the device [22]. Being able to estimate the temperature at different points of the layers of the switch, it requires knowledge of the material characteristics of the individual layers to be set. The Foster model is a more efficient thermal model that just consider the whole system as a partial-fraction RC circuit that estimates the junction

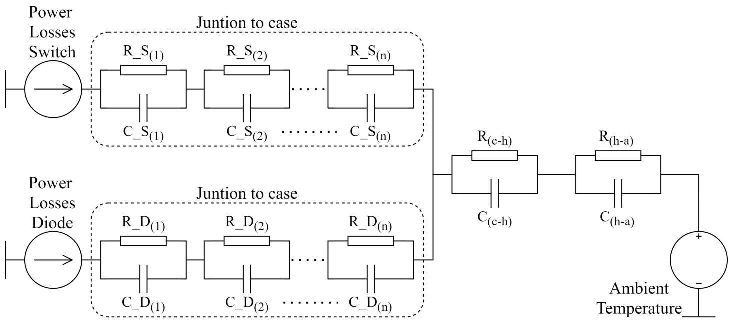

Figure 3: Foster thermal equivalent model of the IGBT devices utilized in this work

temperature but does not represent the true temperature of the other layers of the device [22]. As it can be conveniently extracted from a measured cooling curve of a device, this model is widely used in datasheets. Moreover, with the aim of simplicity and reduced computing time, a Foster model is used in this work, where the thermal parameters for the model are obtained from [23]. The Foster model is shown in Fig. 3. Each of the IGBT and diode have an individual current source to represent their power losses, and a certain number (n) of individual RC elements for the junction to case section ($j-c$) [24]. Afterwards, both layers merge in the case to heat-sink ($c-h$) section, the model continues to the heat-sink to ambient ($h-a$) section and finally, a DC source takes place to represent the ambient temperature.

2.1.3 Rainflow counting

The temperature profile is evaluated with a rainflow algorithm which is a cycle counting technique [19]. The rainflow counting algorithm is a widely used technique in lifetime estimation and stress analysis of thermal cycling [11]. With its application, a random temperature profile which might be difficult to evaluate is transformed into an organized data set that considers the mean junction temperature (T_j), along with the temperature differential (ΔT_j) and cycle period (T_{on}). Afterwards, the number of cycles necessary to failure (N_f) are estimated based on the temperature parameters mentioned and then compared with the number of cycles occurred to estimate the life consumption.

There are two types of temperature cycles in grid-connected PV systems [7]: long-term and short-term temperature cycles. Long-term temperature cycles vary from the second to the year time period and are caused by environmental factors including irradiance and ambient temperature. Short-term temperature cycles are in the range of miliseconds and are caused by the sinusoidal current injection of the power converter and matches with the fundamental frequency of the converter. A representation of long-term (in the second period) and short-term temperature cycles of a IGBT module under an irradiance increment can be seen from the data in Fig. 4.

2.1.4 Lifetime modelling

Empirical models for bond wire fatigue damage are based on experience and data collected from experimentation and are used to calculate the lifetime of power converters. Furthermore, the evaluation of lifetime of power electronics can be modelled by empirical models analyzing the thermal characteristics caused by power cycling during operation [9], where the number of cycles to failure is estimated. Based on accelerated cycling test, these models estimate the number of cycles to failure for power devices under specific mission profiles. Bayerers model [18] is one of these models.

These tools can be used to accurately estimate and compare the lifetime of power converters as they consider different thermal factors, thus, providing the opportunity to find strategies to improve the life of power converters. The model proposed in [18] expresses the number of cycles necessary to cause failure (N_f), by considering the impact on bond wires from mean junction temperature (T_j), junction temperature differential (ΔT_j), cycle heating time (T_{on}) using fitting parameters A, β_1, β_2, β_3 (See Table 1), as shown below:

$$N_f = A \cdot \Delta T_j^{\beta_1} \cdot exp\left(\frac{\beta_2}{T_j + 273}\right) \cdot T_{on}^{\beta_3} \tag{4}$$

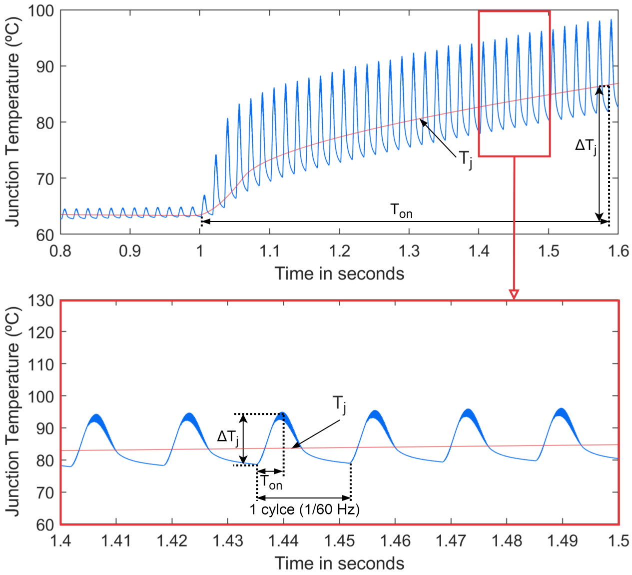

Figure 4: Example of the temperature cycling experienced by an IGBT device during a change in irradiance conditions. Short-term temperature cycle can be seen in the zoomed area. T_j-Mean junction temperature, ΔT_j-Temperature differential, T_{on}- Heating time of the power cycling

Parameter	Value
A	$9.34e^{-14}$
β_1	-4.416
β_2	1.285
β_3	-0.463

Table 1: Constant parameters of the Bayerer´s model [25]

The temperature data organized by the rainflow counting algorithm is processed with Bayerer's model (eq. (4)) and the number of cycles to failure for different combination of thermal parameters (N_{fi}) is obtained. Then, the number of thermal cycles occurred (n_i) and number of cycles to failure (N_{fi}) are compared with the use of Miner's rule (eq. (5)) in order to obtain the life consumption (LC) for the given mission profile. The Miner's rule is linear and is used to accumulate the damage caused by several thermal cycles with different characteristics. This is a commonly used method for comparing the accumulated damage in different scenarios, and it has been validated experimentally in [26] and [27] that the accuracy of this reliability evaluation approach is acceptable in most cases [8].

Here, when $LC \geq 1$ the end of life is reached [28].

$$LC = \sum_i \frac{n_i}{N_{fi}} \tag{5}$$

2.1.5 Reducing computation time for long-term simulation periods using lookup tables

In this work, the operation of a PV converter was simulated for full daylight periods, as explained in Section 3.3. The indicated simulation is extremely time consuming, and the time required to run such simulation would be too extensive. Hence, Lookup Tables (LUTs) were employed to shorten the simulation time. Lookup tables are tools employed to reduce computation time with the use of pre-calculated data and to help with the translation of long-term mission profiles into the desired values. The LUTs in this work are used as a tool to estimate the performance of the MPPT algorithm on the PV converter under different cloud condition irradiance profiles. Moreover, using LUTs, it is possible to have a faster estimate for the life consumption and the energy generated by a PV converter, with good accuracy. For this purpose, two 2-D Lookup tables have been created for each application (Normal and temperature-controlled MPPTs), one of which is assigned to estimate the energy generation while the other one estimates the life consumption.

For this study, the LUTs data was obtained from the operation of the PV converter under a range of irradiance changes explained in Section 3.2. Considering the current irradiance level ($Irra$) and the differential with the previous value ($\Delta Irra$) the energy generation and life consumption are obtained for one-minute irradiance change profiles. Later on, the 2-D LUTs were implemented as a resource to estimate the energy generated and the life consumption of the converter for the given mission profiles. The inputs of the LUTs for one-minute profile estimation are $Irra$ and $\Delta Irra$ obtained from the test mission profiles, which are detailed in Section 3.3. Once the setup of the LUTs is ready for both normal and temperature-controlled MPPT algorithms, the energy generated and life consumption of the PV system under the irradiance mission profiles are determined.

2.2 Temperature-controlled MPPT

The objective of an MPPT algorithm is to track and harvest the maximum energy possible. When changes in irradiance occur, such as when a cloud is passing, the algorithm adapts the duty cycle to find the maximum power point (MPP) available, the change in power generation causes temperature variations and therefore damage to the switching devices. With the application of a modified algorithm, the damaging thermal stresses can be reduced, with no extra cost.

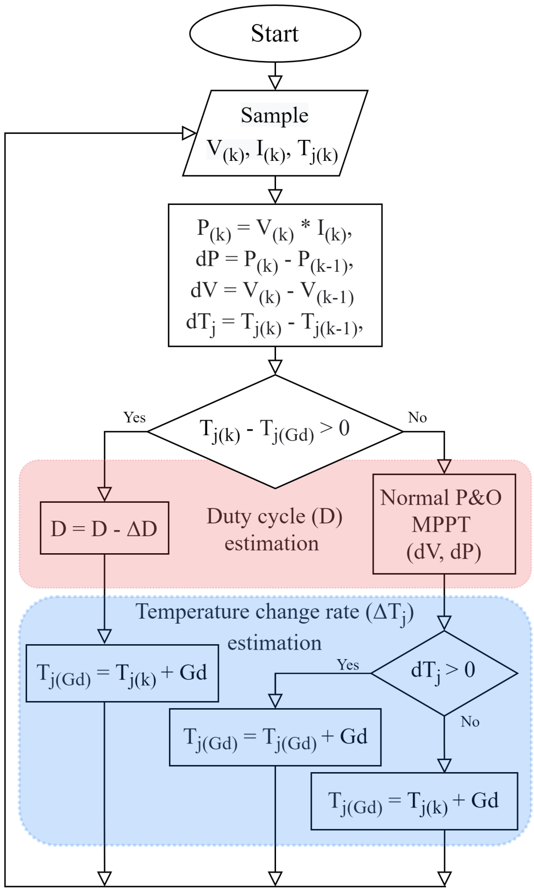

Figure 5: Flow diagram of the proposed temperature-controlled MPPT algorithm. T_j is the junction temperature, V is the voltage, I is the current, P is the power, D is the duty cycle, $T_{j(Gd)}$ is the temperature change rate limit and Gd is the fraction of gradient for each iteration

In this work the effect that dynamic irradiance conditions have on the lifetime of PV system is studied and a temperature-controlled P&O MPPT algorithm is proposed to improve the reliability and lifetime of PV systems under different irradiance variation conditions.This algorithm has the objective of limiting the temperature rate of change of the switches to reduce the impact of T_j and ΔT_j on the switches under dynamic irradiance conditions, such as those experienced in cloudy days. This is achieved with an estimation of the temperature of the IGBT devices and then used by the algorithm to control the temperature changes controlling the duty cycle. If the temperature increases rapidly, the algorithm reduces the duty cycle to limit the rate of temperature change to a preset value.

Furthermore, with the use of the proposed temperature-controlled MPPT algorithm, the temperature rate of change is reduced to the maximum temperature change rate expected during an irradiance change condition. With these reductions in temperature parameters experienced by the system, the lifetime of the IGBT switches can be extended. The lifetime improvement in the IGBT devices can be explained by the high dependency of lifetime on thermal parameters as shown in eq. (4), which suggests even slight reductions in temperature parameters will result in significant high improvements in the lifetime of the switches. However, by modifying the MPPT, the energy production may be negatively affected. Consequently, it is necessary to compare the effectiveness of the modified MPPT algorithm with a normal MPPT algorithm to determine to what extent lifetime improvements outweigh the reduction in energy production under real field irradiance mission profiles for different cloud conditions.

The operation of the temperature-controlled MPPT algorithm can be seen in Fig. 5, where similar to a normal P&O MPPT algorithm the voltage (V) and current (I) are measured at each iteration, with the addition of the determined junction temperature (T_j). The algorithm have two stages, one is used to estimate the duty cycle (D) for the power converter, while the other is used to estimate the temperature change rate limit ($T_{j(Gd)}$) for the next cycle. For both the duty cycle and temperature change rate limit, the present junction temperature is compared with the temperature change rate limit ($T_{j(Gd)}$). If the temperature is increasing faster than the change rate limit (Set to be 3°C/s), (D) is reduced and the new ($T_{j(Gd)}$) is set to the present value of (T_j) plus the fraction of gradient (Gd). In contrast, the normal MPPT algorithm estimates the next duty cycle value and if the temperature is increasing but more slowly than the change rate limit, the new ($T_{j(Gd)}$) is the previous ($T_{j(Gd)}$) plus the fraction of gradient (Gd). If (T_j) is not increasing, the new ($T_{j(Gd)}$) is going to be the present (T_j) plus the fraction of gradient (Gd). The gradient is multiplied by the sample time of the MPPT algorithm to obtain the fraction of gradient (Gd) at each iteration as seen in eq. (6), where T_s is the sample time:

$$Gd = Gradient \times T_s \tag{6}$$

The modified MPPT algorithm is applied to control a boost converter of a two-stage PV converter. For boost converters, the output voltage (V_{out}) is affected by the input voltage (V_{in}) in relation with the duty cycle as seen in equation (7) [34]. With the reduction of the duty cycle, the output voltage is reduced and the output power is limited, limiting the temperature rise of the devices.

$$V_{out} = \frac{V_{in}}{1 - D} \tag{7}$$

As can be seen in Fig. 5, the proposed method is simple, easy to implement and does not need complex calculations. Its effect on the harvested power and lifetime of the converter is studied using computer simulations, as presented in the next section.

3 Simulation and Results

In this section, the lifetime modelling discussed in Section 2.1 is applied to a PV system controlled by the normal MPPT algorithm and another identical system controlled by the proposed temperature-controlled MPPT described in Section 2.2. The studied PV system consists of a PV array and converter which are simulated in Matlab Simulink environment. The PV model is composed of an array of 4 parallel-connected sections of 10 series-connected modules each, with the module from Trina solar manufacturer [29] (See Table 2 for characteristics), reaching a rated power of 10 kW under standard test conditions (STC). The parameters of the PV converter can be seen in Table 3, a relatively low switching frequency (3kHz) has been deliberately chosen to show that even with low switching frequency and therefore lower thermal stress, the modified algorithm is able to improve the reliability of the PV system.

The switching devices used in the model are five IKW50N60H3 IGBT from Infineon [23], one of which is used for the boost converter and the remaining four in the H-bridge converter. Moreover, the heat sink is designed to ensure that a maximum junction temperature ($T_{j,max}$) of 150°C is never reached under the expected mission profile. The ambient temperature has been set to be constant at 25°C to make the effect that solar irradiance has in the lifetime of the system clearer.

The parameters of the foster model are listed in Table 5. Note that the capacitance values for the foster model are not provided directly, and therefore it is necessary to calculate them using:

$$C_n = \tau_n / R_n \tag{8}$$

Description	Parameter	Value
Panel power	Pmp	250 W
Open circuit voltage	Voc	37.6 V
Voltage at maximum power point	Vmp	31.0 V
Short-circuit current	Isc	8.85 A
Current at maximum power point	Imp	8.06 A

Table 2: Electrical parameters of the 250W Trina Solar PV Panel at Standard Test Conditions (STC) values

Description	Parameter	Value
Two-stage PV converter		
Rated power		10 kW
Grid frequency		60 Hz
Grid voltage	(RMS)	240 V
Switching frequency	f	3 kHz
Boost converter		
Inductor	L	$1.3mH$
PV capacitor	Cpv	$1000\mu F$
DC-link capacitor	Cdc	$1500\mu F$
LCL filter		
Inverter side inductor	Linv	$3.6mH$
Grid side inductor	Lg	$8.6mH$
Capactior	Cf	$9.5\mu F$

Table 3: Electrical parameters of the 2-stage 10kW PV converter

where C_n is the thermal capacitance value, τ_n is the thermal time constant and R_n is the thermal resistance.

The parameters necessary for power losses estimation can be extracted directly from the datasheet at the highest T_j to represent the worst-case scenario. These parameters can be seen in Table 4.

Table 4: Parameters for the power losses calculation

Description	Parameter	Value
IGBT		
On-state resistance	R_{on}	0.0222Ω
Turn-on energy	E_{on}	$1.42mJ$
Turn-off energy	E_{off}	$1.13mJ$
Diode		
On-state resistance	R_D	0.0179Ω
Reverse recovery energy	E_{rec}	$0.96mJ$

The results of both algorithms are compared to determine to what extent the temperature-controlled algorithm is able to improve the lifetime of a PV converter without compromising the energy generation. For the collection of data to compare both algorithms, a simulation of the converter for the complete daily irradiance profiles is required, where simulations would be very time-consuming. Therefore, as mentioned in Section 2.1.5 the application of Lookup Tables (LUTs) has been chosen to reduce the simulation time whilst maintaining accuracy.

3.1 Temperature change rate limitation

In order to validate the functioning of the algorithm, the temperature limitation is tested first. The temperature gradient selected for this paper is 3°C/s, however this value might be modified for other systems and for achieving faster dynamics or lower lifetime consumption. An irradiance change with short rise time (30s) from 100 W/m^2 to 1000 W/m^2 is applied to the converter and its effect on the switch junction temperature can be seen in Fig. 6.

Table 5: IGBT and diode thermal parameters for the foster thermal model

Impedance		$Z_{th(j-c)}$					$Z_{th(c-h)}$
	n	1	2	3	4	5	
IGBT	R_n (K/W)	7.0e-3	0.037	0.092	0.130	0.183	0.7
	τ_n (s)	4.4e-5	1.0e-4	7.2e-4	8.3e-3	0.074	0.25
Diode	R_n (K/W)	0.049	0.225	0.313	0.268	0.195	0.7
	τ_n (s)	7.5e-6	2.2e-4	2.3e-3	0.015	0.107	0.25

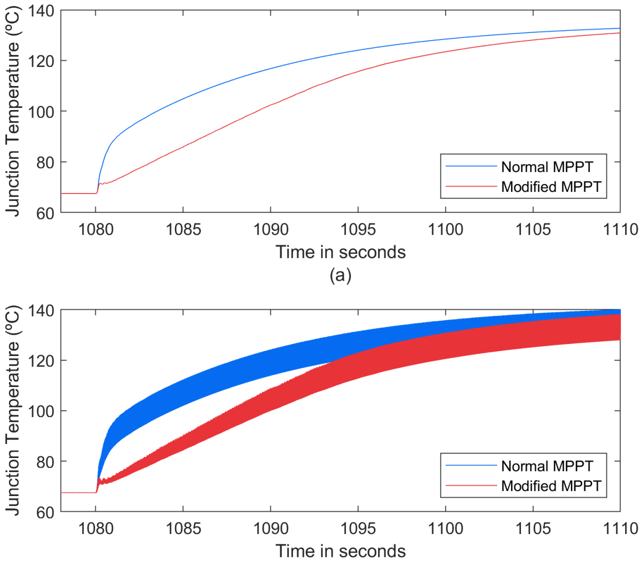

Figure 6: Comparison of the application of the modified and a normal MPPT algorithm of the mean junction temperature (a), and temperature differential (b) of a switch for an irradiance change from 100 W/m^2 to 1000 W/m^2.

The data in Fig. 6(a) show the effect of the algorithm on the mean junction temperature (T_j) and Fig. 6(b) shows the junction temperature differential (ΔT_J) respectively. The use of the proposed algorithm leads to a reduction in thermal stress as the T_j took 5 s longer to reach 100°C (Fig. 6(a)) and the ΔT_J is lower for more than 10 s (Fig. 6(b)) during the increasing irradiance change. For further comparison, the rainflow counting histogram of normal and temperature-controlled algorithm can be seen in Fig. 7 and Fig. 8 respectively. The proposed algorithm results in overall lower junction temperature, which according to the equation (4) in turn results in the improvement of the lifetime of the system.

3.2 Irradiance mission profile (Training data) and lifetime modelling

In order to obtain a base data set and test the effectiveness of the proposed algorithm, an irradiance profile has been designed. This profile is then applied to both normal and temperature-controlled MPPT systems to test them as well as to collect the data required to populate the 2-D Lookup tables. To obtain a base data set for the LUTs, the proposed irradiance profile shown in Fig. 9 is fed to both simulations. Small scale irradiance fluctuations have little impact in PV applications [16] while large scale fluctuations ($\Delta Irradiance > 100\text{W/m}^2$) need to be studied . The proposed mission profile is composed of 100 minutes of irradiance in one-minute periods and comprises all possible fluctuations of irradiance values, where the irradiance values are all multiples of 100 W/m^2 from a range of 100 to 1000 W/m^2. Other irradiance fluctuations in between these values are mathematically estimated by interpolation by the LUTs. From the proposed irradiance profile, the input values of the LUTs are obtained, where the first input is the current irradiance (Irr) value and the second input is the differential with the previous irradiance value (ΔIrr).

The proposed mission profile is applied to the previously described 10kW converter under the control of both normal and temperature-controlled MPPT algorithms. From the electrical model the total energy generated is obtained in discrete minute intervals to be used as the references values of the LUTs.

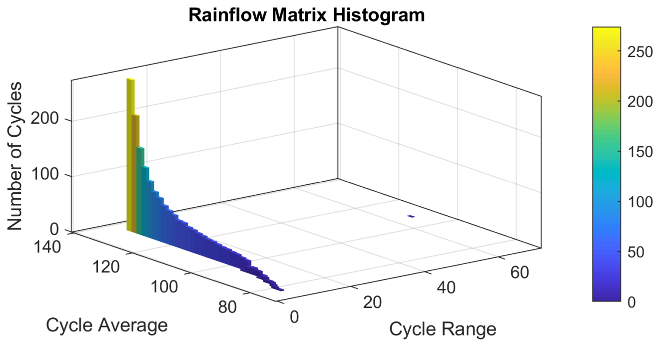

Figure 7: Rainflow counting of the temperature cycles for an irradiance change from 100 W/m^2 to 1000 W/m^2 under a normal MPPT algorithm

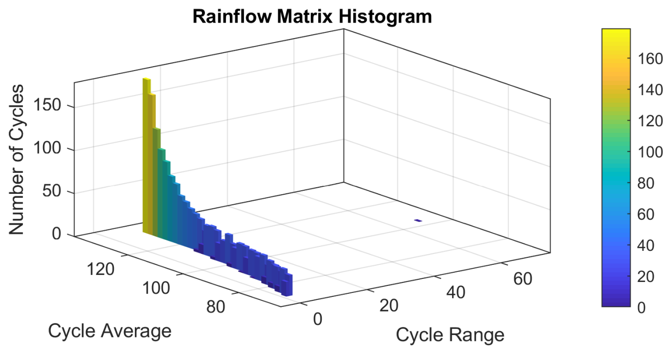

Figure 8: Rainflow counting of the temperature cycles for an irradiance change from 100 W/m^2 to 1000 W/m^2 under the proposed temperature-controlled MPPT algorithm

Furthermore, the electrical parameters of an IGBT is extracted and the switching losses determined. These losses are then fed to the foster thermal equivalent model to estimate the junction temperature of the switching device during the mission profile. Afterwards, the temperature cycles are counted and separate by a rainflow counting algorithm and the lifetime estimation technique is applied to estimate the life consumption.

Besides, all the above process is broken up in the individual minute profiles to get the output data for the LUTs, which are rearranged in 10 by 10 LUTs that comprise of the 100 minutes of the proposed mission profile. These are then used to give an estimation of the energy generated and damaged received by the converter under the daily irradiance mission profiles under different cloud conditions. The comparison of the total energy generated and total life consumption for the mission profile under both MPPT algorithms can be observed in Fig. 10(a) and Fig. 10(b) respectively. It is important to notice from the comparison between strategies that in Fig. 10(a) the reduction of generated energy is negligible from 8.742 kWh to 8.711 kWh (0.35% reduction), while in Fig. 10(b) the damage reduction is noticeable from 2.937 e^{-05} to 2.575 e^{-05} (12.24% reduction).

For the verification of the LUTs performance, a solar irradiance mission profile was designed (See Fig. 11) to evaluate their accuracy. The mission profile is composed of 20 minutes of solar irradiance, the PV system is tested with the mentioned mission profile. Then, the irradiance profile is also processed by the LUTs. The energy generated and life consumption (Fig. 12 (a) and (b)) are obtained from simulation results and LUT estimation each. Then these results are compared to determine the accuracy of the LUTs which is 95.34% for the estimation of the life consumption, and 99.9% for the estimation of the energy generated.

3.3 Irradiance mission profile (Test data)

Now that the application of the algorithm has shown its effectiveness under a designed irradiance mission profile, the algorithm is applied to daily irradiance mission profiles, to find to what extent its application is effective in reducing the life consumption of the converter, while observing its effect on the energy yield of the system. As the simulation of the the mission profiles in this subsection would be really

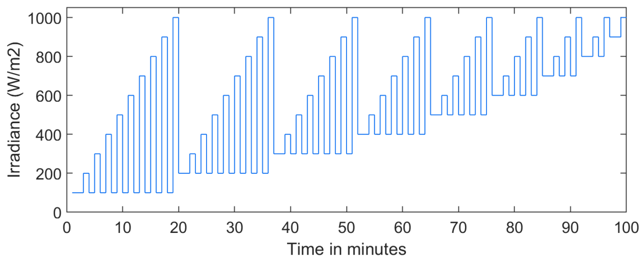

Figure 9: Irradiance profile proposal for the data obtainting for the LUT. With irradiance levels multiple of 100 W/m^2 and short ramp times in between irradiance levels

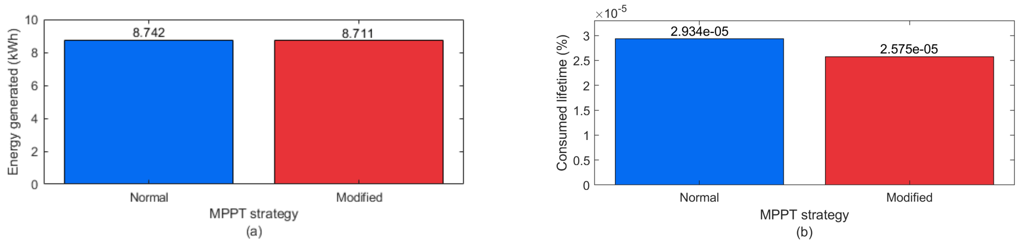

Figure 10: Comparison of the energy generated (a) and life consumption (b) of the system under the proposed irradiance mission profile for normal and temperature-controlled MPPT algorithm

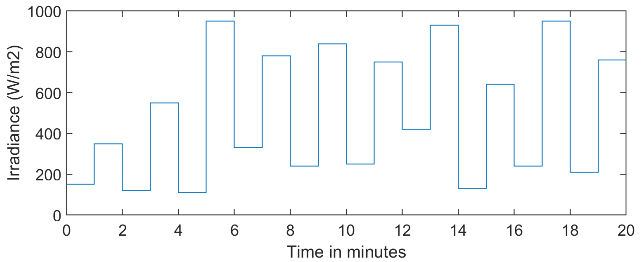

Figure 11: Irradiance profile to test the performance of the LUTs

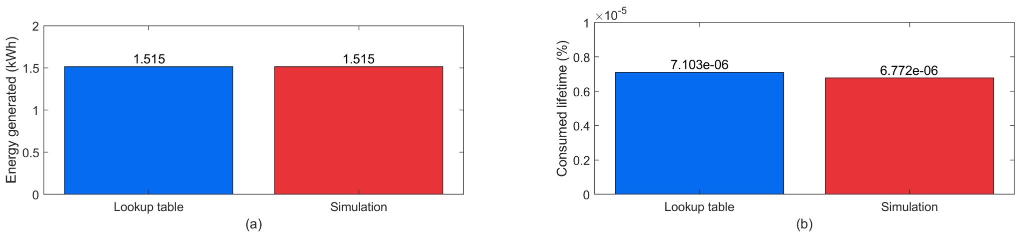

Figure 12: Example of the energy generated (a) and life consumption (b) obtained with the use of the LUTs compared with the results obtained directly from simulation for the normal MPPT algorithm with a 20 min test irradiance profile

time consuming, the validated LUT tables from above are applied here to accurately estimate the life consumption and energy generated by the PV system.

To this end, four different irradiance data sets are used to feed the LUTs and the generated energy and life consumption of the converter are determined for each of them. The data sets used in this work are from the province of Quebec, Canada [30]. To obtain the irradiance data sets, very precise irradiance sensors were used to allow the millisecond sample rate. To reduce the size of the data sets, recording of data is limited to a resolution sample rate of 1 second if at least 5 W/m^2 change in the data is observed, otherwise the irradiance is recorded every minute [30]. The data sets represent four different type of cloud conditions: clear sky, overcast, variable and very variable as shown in Fig. 13. To have regular intervals that allow consistent comparison of data between different cloud conditions, just the one-minute

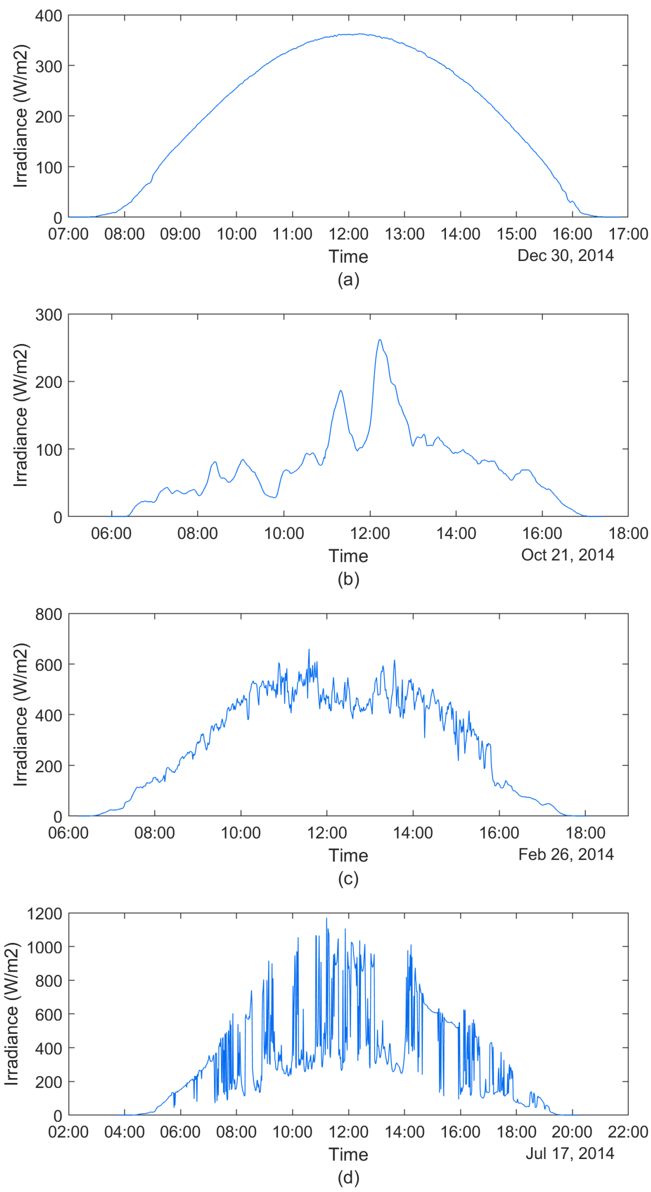

Figure 13: Irradiance profiles during days for clear sky (a), overcast (b), variable (c) and very variable (d) cloud conditions in the province of Quebec, Canada.

data samples are used in this work.

The temperature-controlled MPPT algorithm is compared with the application of a normal MPPT algorithm under the same irradiance conditions. The life consumption is calculated with the application of the trained LUTs on the cloud conditions irradiance profiles, the accumulated consumed lifetime can be seen in Fig. 14. The energy generated and the life consumption are compared between both algorithms as seen in Fig. 15(a) and Fig. 15(b) respectively.

For the clear sky conditions, overcast and variable cloud conditions, the algorithm has a negligible effect in life consumption (Fig. 14(a-c)), as further explained in the next paragraphs. However, there is a considerable effect on the life consumption reduction for the very variable cloud conditions (Fig. 14(d)), which means that for a day with very variable cloud conditions, the life consumption of the converter can be reduced 4.68% with an energy reduction of only around 0.08% (See table 4). This shows that for very variable cloud conditions, by simply modifying the MPPT algorithm as proposed here, it is possible to considerably decrease the life consumption at the cost of only a negligible drop in the harvested power.

The MPPT algorithm applied in this work has shown good performance under very variable cloud conditions, where the irradiance changes are fast and large, while for the rest of cloud conditions have shown minor or no effect. The changes in irradiance can occur in between low, medium and high

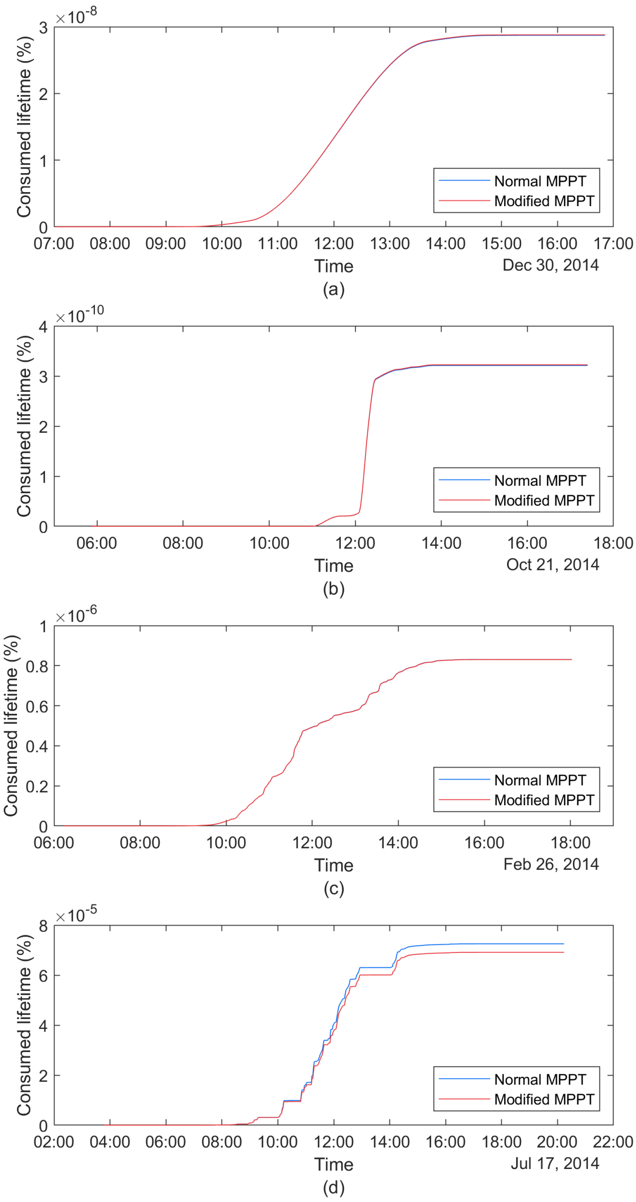

Figure 14: Accumulated life consumption of the PV inverter under one day mission profile for clear sky (a), overcast (b), variable (c) and very variable (d) cloud conditions

irradiance levels. The irradiance changes from low to high levels are those with the highest potential for lifetime improvement. Low to medium and medium to high irradiance changes have a lower potential of lifetime improvement. Moreover, the electric characteristics of silicon PV modules for the array applied in this work can be seen in Fig. 16. It shows that the MPP voltage for medium (0.4 to 0.7 kW/m^2) and high (0.8 to 1 kW/m^2) irradiance levels is similar being around 310 V, while for low (0.1 to 0.3 kW/m^2) irradiance levels voltages are lower and different for each case. With similar input voltage values, the duty cycle necessary to reach the MPP will be almost identical. As the temperature-controlled MPPT algorithm works by controlling the duty cycle, the algorithm has little effect for changes on irradiance from 0.4 to 1 kW/m^2 irradiance levels. This explains why the algorithm has no appreciable effect on overcast and variable cloud conditions. This is different for the very variable days that have higher irradiance changes, including changes from low to high irradiance levels. Overall, it is demonstrated that the application of the proposed temperature-controlled algorithm can result in an improved lifetime and reliability of a PV system with a limited impact in its energy production. Moreover, the study of the proposed algorithm shows its applicability for PV systems that experience variable irradiance conditions, at no extra cost.

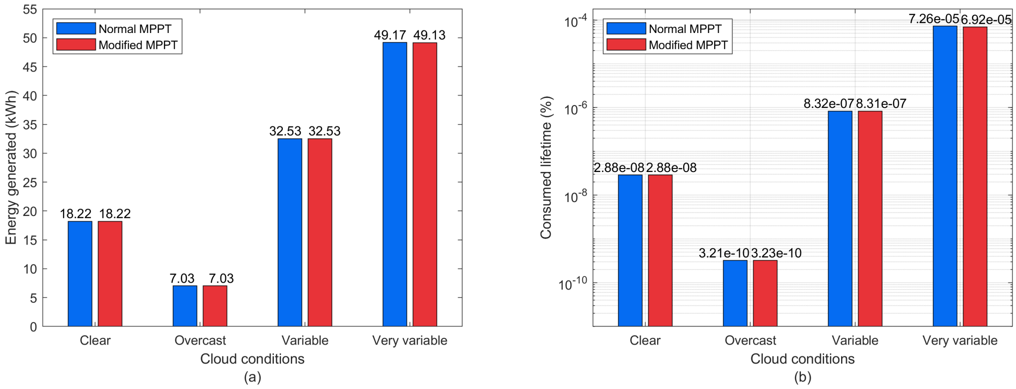

Figure 15: Comparison of the energy generated (a) and life consumption (b) of the PV converter under different cloud conditions under both normal and temperature-controlled MPPT algorithm

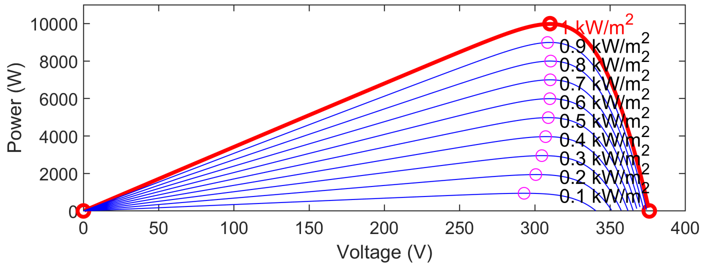

Figure 16: Electrical performance of a PV array of 10 series modules and 4 parallel strings with solar modules of 250W. Maximum power points values for different irradiance levels are in pink circles.

3.4 Discussion of results and comparison with related works

As discussed in the introduction, while there has been a huge number of works on MPPT algorithm [31][32], very few papers have addressed reliability improvement for MPPT schemes. Furthermore, while many of those works have studied variable cloud conditions from MPPT point of view, the study of different cloud conditions (including highly variable could conditions) on lifetime consumption and reliability of power converters in PV systems is not done before, to the best of authors knowledge. A power limited control is discussed in [8] that limits the extracted power of the solar cells to the rated power, in case the available PV power becomes larger than the converter's rated power (this can happen in PV systems with oversized PV arrays, or due to solar irradiance reflection from the clouds). Other relevant works have studied reliability improvement also have the same problem. Examples are [1] where the effect of panel selection and phase shift PWM in parallel converters reliability is studied, however the MPPT is not part of this study, and [33] which presents another control strategy that works by limiting the output power of the inverter/panels. However, none of these strategies have considered variable cloud/irradiance conditions and would make little or no improvements during those conditions. [15] proposed an MPPT method for damage reduction by trying to limit the positive temperature gradient and the maximum junction temperature of the semiconductors. Only a relatively short (620s) section of a daily mission profile is considered for verification purposes, while the mission profile is extremely important in the reliability assessment and lifetime prediction of PV inverters. Our work, however, has evaluated the impact that the implementation of our proposed algorithm would have in field applications (by considering different irradiance conditions) which is crucial in determining its effectiveness in real situations. Moreover, the algorithm proposed in our work is simpler compared to the one in [15], and also it relies on fewer steps to achieve temperature control of the switching devices, making it more suitable for practical implementation, and for a wider range of existing MPPT methods.

Nevertheless, it is worth mentioning that the proposed approach is designed by modifying the P&O method, and therefore is limited by its potential drawbacks. Several advanced MPPT methods are proposed in the literature in recent years, some of which may present better performance compared with

	MPPT strategy	Clear sky	Overcast	Variable	Very variable
EG(kWh)	Normal	18.22	7.03	32.53	49.17
	Modified	18.22	7.03	32.53	49.13
LC(%)	Normal	2.88e-08	3.21e-10	8.32e-07	7.26e-05
	Modified	2.88e-08	3.23e-10	8.31e-07	6.92e-05

Table 6: Comparison of normal and the controlled MPPT algorithm effects on the energy generated and the life consumption of the converter under different cloud conditions. EG is the energy generated and LC is the life consumption.

P&O in terms of efficiency or steady-state oscillation. [31][32]. The main reason for selecting the P&O method is its low cost and complexity and therefore the widespread use of this method, and also the fact that hill climbing methods such as P&O are found in previous studies to cause least thermal stress for the power semiconductors [15]. However we would like to point out that at the same time, this work can also benefit from future progress in P&O methods. Also, further development can be done by modification of other MPPT approaches in the future research.

Also, as it was shown by the results, the proposed method will result in a decrease in the power generation, however this reduction in power generation is shown to be small, and in fact negligible compared to the increase in the converter's lifetime.

4 Conclusions

In this paper, the lifetime of a PV system has been evaluated under different dynamic irradiance conditions and a temperature-controlled MPPT algorithm is proposed and applied to improve the lifetime of PV systems under these irradiance conditions. The performance of the algorithm has been tested under four irradiance mission profiles for different cloud conditions. The modified algorithm has shown its capability in limiting the temperature change rate during highly dynamic irradiance conditions, thus, reducing the life consumption of the IGBTs without compromising the energy generation. The effectiveness of the proposed algorithm is verified using by comparing energy generated and life consumption under irradiance profiles for different cloud conditions. The temperature-controlled algorithm is applied in parallel with a normal MPPT algorithm to a 10 kW photovoltaic system using irradiance data from the province of Quebec, Canada. The study showed that for days with very variable cloud conditions, the algorithm can reduce the life consumption by 4.68% with just 0.08% of energy reduction, and at no other extra cost.

The latitude of the province of Quebec, Canada has a noticeable effect on the irradiance levels for the days with low cloud conditions, being these in the range of low and medium irradiance levels for the days with a clear sky, overcast and variable cloud conditions. Therefore, the performance of the algorithm may improve in locations closer to the equator, which is going to be the subject of further study.

Also, the proposed approach is designed by modifying the P&O method, and therefore is limited by its potential drawbacks, while it can also benefit from future progress in this method. While the reason for selecting the P&O method was its low cost and complexity and therefore its widespread use, several other advanced MPPT methods are proposed in the literature in recent years, some of which may present better performance compared with P&O in terms of efficiency or steady-state oscillation, and therefore further development can be done by modification of other MPPT approaches for improved reliability in the future research.

References

[1] Peyghami, Saeed, et al. "System-level reliability enhancement of DC/DC stage in a single-phase PV inverter." Microelectronics Reliability 88 (2018): 1030-1035.

[2] João Victor M. Farias, Allan F. Cupertino, Victor de Nazareth Ferreira, Heverton A. Pereira,and Seleme Isaac Seleme. "Redundancy design for modular multilevel converter based statcoms", Microelectronics Reliability, 100 (2019): 113471.

[3] HuaLu, Chris Bailey, Chunyan Yin, Microelectronics Reliability, "Design for reliability of power electronics modules", Microelectronics Reliability Volume 49, Issues 9–11, September–November 2009, Pages 1250-1255.

[4] H. Wang, K. Ma and F. Blaabjerg, "Design for reliability of power electronic systems," IECON 2012 - 38th Annual Conference on IEEE Industrial Electronics Society, Montreal, QC, pp. 33-44 2012.

[5] H. Wang, M. Liserre and F. Blaabjerg, "Toward Reliable Power Electronics: Challenges, Design Tools and Opportunities," IEEE Industrial Electronics Magazine, vol.7, no.2, pp.17-26, June 2013.

[6] J. Falck, C. Felgemacher, A. Rojko, M. Liserre and P. Zacharias, "Reliability of Power Electronic Systems: An Industry Perspective," IEEE Industrial Electronics Magazine, vol. 12, no. 2, pp. 24-35, June 2018.

[7] H.S. Chung, H. Wang, F. Blaabjerg, and M. Pecht, "Reliability of power electronic converter systems," Energy Engineering, Institution of Engineering and Technology, 2015, Chap. 13.

[8] A. Sangwongwanich, Y. Yang, D. Sera and F. Blaabjerg, "Mission Profile-Oriented Control for Reliability and Lifetime of Photovoltaic Inverters," in IEEE Transactions on Industry Applications, vol. 56, no. 1, pp. 601-610, Jan.-Feb. 2020

[9] Fogsgaard, Martin Bendix, et al. "PV mission profile simplification method for power devices subjected to arid climates." Microelectronics Reliability (2021): 114328.

[10] Mauro Ciappa, "Selected failure mechanisms of modern power modules", Microelectronics Reliability, Volume 42, Issues 4–5, April–May 2002, Pages 653-667

[11] A. Sangwongwanich, Y. Yang, D. Sera and F. Blaabjerg, "Lifetime Evaluation of Grid-Connected PV Inverters Considering Panel Degradation Rates and Installation Sites," IEEE Transactions on Power Electronics, vol. 33, no. 2, pp. 1225-1236, Feb. 2018.

[12] T. Tomson, "Fast dynamic processes of solar radiation," Solar Energy, vol. 84, no. 2, pp. 318–323, 2010.

[13] A. Sangwongwanich, Y. Yang, D. Sera and F. Blaabjerg , "On the Impacts of PV Array Sizing on the Inverter Reliability and Lifetime," IEEE Transactions on Industry Applications, vol. 54, no. 4, pp. 3656-3667, July-Aug. 2018.

[14] Markus Andresen Giampaolo Buticchi Marco Liserre, "Study of reliability-efficiency tradeoff of active thermal control for power electronic systemsMicroelectronics Reliability", Microelectronics Reliability, Volume 58, March 2016, Pages 119-125.

[15] M. Andresen, G. Buticchi and M. Liserre "Thermal Stress Analysis and MPPT Optimization of Photovoltaic Systems" IEEE Transactions on Industrial Electronics, vol.63, no.8, pp.4889-4898, 2016.

[16] T. Tomson, "Fast dynamic processes of solar radiation" Solar Energy, vol.84, no.2, pp.318–323, 2010.

[17] P. D. Reigosa, H. Wang, Y. Yang and F. Blaabjerb, "Prediction of Bond Wire Fatigue of IGBTs in a PV Inverter Under a Long-Term Operation," IEEE Transactions on Power Electronics, vol. 31, no. 10, pp. 7171-7182, Oct. 2016.

[18] R. Bayerer, T. Herrmann, T. Licht, j. Lutz and M. Feller, "Model for Power Cycling lifetime of IGBT Modules - various factors influencing lifetime," in 5th International Conference on Integrated Power Electronics Systems, 2008, pp. 1-6.

[19] M. Musallam, C.M. Johnson, "An Efficient Implementation of the Rainflow Counting algorithm for Life Consumption Estimation," IEEE Transaction on Reliability, vol.61, no.4, pp.978-986, Dec.2012.

[20] Rashid, Muhammad H., ed. Power electronics handbook. Chapter 14: Inverters, Butterworth-Heinemann, 2017.

[21] Yazdani, Amirnaser, and Reza Iravani. Voltage-sourced converters in power systems: modeling, control, and applications. John Wiley & Sons, 2010.

[22] Infineon Technologies AG, "Transient Thermal Measurements and thermal equivalent circuit models", Munich, Germany, 2015, [Online]. Available: https://www.infineon.com/dgdl/Infineon-Thermal_equivalent_circuit_models-ApplicationNotes-v01_02-EN.pdf?fileId=db3a30431a5c32f2011aa65358394dd2

[23] Infineon Technologies AG, "IKW50N60H3", Munich, Germany, 2014, [Online]. Available: https://www.infineon.com/dgdl/Infineon-IKW50N60H3-DataSheet-v02_02-EN.pdf?fileId=db3a30432a40a650012a47934b1e2bea

[24] Infineon Technologies AG, "Transient Thermal Measurements and thermal equivalent circuit models", Munich, Germany, 2015, [Online]. Available: https://www.infineon.com/dgdl/Infineon-Thermal_equivalent_circuit_models-ApplicationNotes-v01_02-EN.pdf?fileId=db3a30431a5c32f2011aa65358394dd2

[25] R. Bayerer, T. Herrmann, T. Licht, j. Lutz and M. Feller, "Model for Power Cycling lifetime of IGBT Modules - various factors influencing lifetime," in 5th International Conference on Integrated Power Electronics Systems, 2008, pp. 1-6.

[26] U. M. Choi, K. Ma, and F. Blaabjerg, "Validation of lifetime prediction of IGBT modules based on linear damage accumulation by means of superimposed power cycling tests," IEEE Trans. Ind. Electron., vol. 65, no. 4, pp. 3520–3529, Apr. 2018.

[27] G. Zeng, C. Herold, T. Methfessel, M. Schafer, O. Schilling, and J.Lutz,"Experimental investigation of linear cumulative damage theory with power cycling test," IEEE Trans. Power Electron., vol. 34, no. 5, pp. 4722– 4728, May 2019.

[28] M. A. Miner, "Cumulative damage in fatigue," Journal of applied Mechanics. Trans.ASME, vol. 12, pp. A159-A164, 1945.

[29] "TSM-PC05 Datasheet," Trina Solar, Nov. 2012. [Online]. Available: https://static.trinasolar.com/sites/default/files/PC05_Datasheet_40mm_EN.pdf

[30] "High-Resolution Solar Radiation Datasets," Government of Canada, Feb. 18, 2020. Accessed on: Jun. 14, 2020.[Online]. Available: Available: https://www.nrcan.gc.ca/energy/renewable-electricity/solar-photovoltaic/18409

[31] Li, Xingshuo, et al. "A comparative study on photovoltaic MPPT algorithms under EN50530 dynamic test procedure." IEEE Transactions on Power Electronics 36.4, 4153-4168, 2020.

[32] Hanzaei, Saeed H., Saman A. Gorji, and Mehran Ektesabi. "A scheme-based review of MPPT techniques with respect to input variables including solar irradiance and PV arrays' temperature." IEEE Access 8, 182229-182239, 2020.

[33] Yang, Yongheng, et al. "Pursuing photovoltaic cost-effectiveness: Absolute active power control offers hope in single-phase PV systems." IEEE Industry Applications Magazine 23.5, 40-49, 2017.

[34] "Basic Calculation of a Boost Converter's Power Stage," Texas Instruments, Jan, 2014. Accessed on: Feb. 11, 2021.[Online]. Available: Available: https://www.ti.com/lit/an/slva372c/slva372c.pdf?ts=1613010991603